

Weighing the Axion with Muon Haloscopy

N. Bray-Ali*
Science Synergy,
Los Angeles, CA 90045
 (Dated: March 18, 2024)

Recent measurements of muon spin precession confirm a long-standing tension with the standard model of particle physics. We argue that axions form the dark matter in the universe and that axions from the local dark matter halo of the galaxy are responsible for the tension. The argument gives a percent level prediction for the mass of the axion that can be tested by measuring the mid-infrared electrodynamic response of a wide range of polar materials. A broad resonance in the scattered visible light intensity from quartz crystal at room-temperature and ambient pressure is reported that peaks at a frequency shift of the light which is consistent with the creation of axions with the predicted mass.

Introduction—The spin of the muon precesses in a magnetic field B at frequency $\omega_a = a_\mu(e/m_\mu)B$, where, $a_\mu \approx \alpha/(2\pi) \approx 1.16 \times 10^{-3}$ is the electromagnetic leading order contribution to spin precession, and $e/m_\mu = 2\pi \times 135$ MHz/T is the charge to mass ratio of the muon [1–5]. In this Letter, we show that axions in the local dark matter halo of the galaxy shift a_μ from the standard model value. The demonstration rests on a novel physical picture for the nature of dark matter which leads to a percent level prediction for the mass of the axion.

Nature of Dark Matter—We start by expressing the axion A_M in terms of quarks and leptons M_H^P with helicity $H = L, R$ and charge-parity check $P = +, -$ [6]:

$$A_M = M_L^- \bar{M}_R^- - M_R^+ \bar{M}_L^+ - M_L^+ \bar{M}_R^+ + M_R^- \bar{M}_L^- \quad (1)$$

Here, M runs over the twelve known “flavors” of quarks and leptons while the charge-parity check P is $+$ for quarks and leptons that do not feel the weak nuclear force and $-$ for those that do. In the standard model, we find M_L^- and M_R^+ , but neither M_L^+ nor M_R^- , where, L is for left-handed and R is for right-handed helicity [7].

Next, we suppose that axions A_M of each kind and photons γ_H of each helicity formed in equal numbers in the early universe prior to baryogenesis. This fixes the ratio $n_A/n_\gamma = |M|/|H| = 6$ of axions to photons and gives the axion rest-mass energy [8]:

$$m_A c^2 = 2.70 kT_\gamma \left(\frac{n_A}{n_\gamma} \right)^{-1} \frac{\Omega_A h^2}{\Omega_\gamma h^2} = (0.508 \pm 0.004) \text{ eV}, \quad (2)$$

where, $T_\gamma = (2.7255 \pm 0.0006)$ K is the present photon temperature [9], $\Omega_\gamma h^2 = (2.473 \pm 0.002) \times 10^{-5}$ is the photon energy density parameter and $\Omega_A h^2 = 0.11882 \pm 0.00086$ is that of dark matter [10].

Muon Haloscopy—Figure 1 shows how axions in the local dark matter halo shift muon spin precession [3–5]. Acting as a background field $\tilde{\phi}_A(q_A)$ with on-shell four-momentum $q_A^2 = (m_A c)^2 \ll (m_\mu c)^2$, the axion A couples to the virtual photon dressing the vertex of the positive muon μ^+ and the magnetic field B . The axion-photon

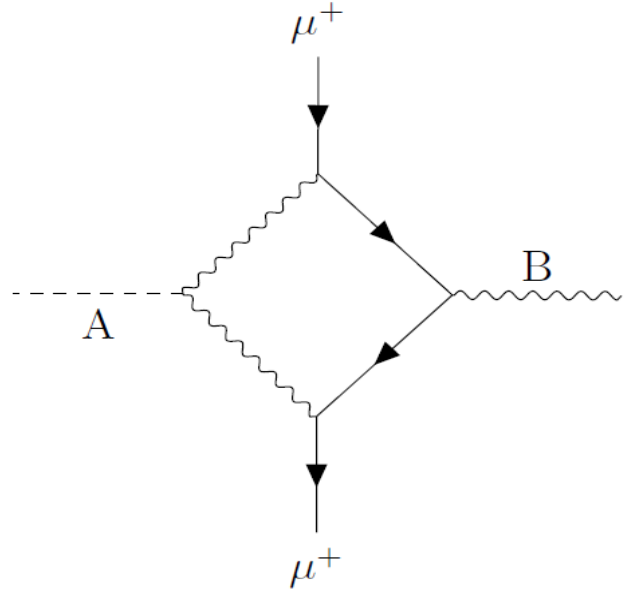


FIG. 1. Halo axion A collides with virtual photon dressing vertex of positive muon μ^+ and magnetic field B .

coupling of strength $g_{A\gamma\gamma} = (0.68 \pm 0.02) \times 10^{-10} \text{ GeV}^{-1}$ [12] changes the photon’s Green’s function [13, 14]

$$\Delta D_+(x, x') = m_A^2 c^4 g_{A\gamma\gamma} \tilde{\phi}(q_A) D_+(x, x'), \quad (3)$$

and this change in the photon propagator produces the shift of the spin precession frequency [15]:

$$\begin{aligned} \frac{\Delta a_\mu}{a_\mu} &= m_A^2 c^4 g_{A\gamma\gamma} \tilde{\phi}_A(q_A) \\ &= \pm m_A c^2 g_{A\gamma\gamma} \sqrt{\rho_A N_\mu V_\mu T_\mu / \hbar} \end{aligned} \quad (4)$$

where, the axion field strength $|\tilde{\phi}_A(q_A)|^2 \approx \phi_A^2 N_\mu V_\mu T_\mu / \hbar$ is fixed by the axion energy density $\rho_A = \phi_A^2 m_A^2 c^4$, the volume V_μ of the muon beam, the lifetime T_μ of the muon in the axion rest-frame, and the average number of muons

N_μ during spin precession. The best astrophysical estimate for the energy density of dark matter in the local halo is $\rho_A = (0.30 \pm 0.03) \text{ GeV/cm}^3$ [16].

The sign of the axion-driven shift Δa_μ of the muon spin precession frequency switches along with the axion field $\phi_A(q_A)$ under spatial inversion P , under time-reversal T , and under the combinations CP and CT with charge conjugation C [17]. The size of the shift scales with muon beam parameters [18]

$$\Delta a_\mu = (171 \pm 10) \times 10^{-11} \left(\frac{N_\mu}{1930} \right)^{1/2} \left(\frac{\sigma_x}{1.78 \text{ cm}} \right)^{1/2} \times \left(\frac{\sigma_y}{1.25 \text{ cm}} \right)^{1/2} \left(\frac{R}{711 \text{ cm}} \right)^{1/2} \left(\frac{T_\mu}{64.4 \text{ } \mu\text{sec}} \right)^{1/2} \quad (5)$$

where, σ_x is the width of the muon beam, σ_y is its height, and R is the radius of the storage ring. Combining the shifts found from Eq. (6) using the muon beam parameters for the two experiments (FNAL E989 [2, 3] and BNL E821[4]) that dominate the experimental world average $a_\mu(\text{Exp})$, we find the weighted average shift

$$\Delta a_\mu(\text{Exp}) = (171 \pm 10) \times 10^{-11}, \quad (6)$$

where, we have used the same weights for $\Delta a_\mu(\text{Exp})$ as the weights entering $a_\mu(\text{Exp})$ [18]. This shift roughly resolves the 3.4σ tension between $a_\mu(\text{Exp})$ and the standard model value $a_\mu(\text{SM})$ [19–24]:

$$a_\mu(\text{Exp}) - a_\mu(\text{SM}) = (140 \pm 41) \times 10^{-11}, \quad (7)$$

where, we have used the recently emerged consensus value $a_\mu^{\text{HLO}}(\text{SM}) = (704.1 \pm 3.0) \times 10^{-10}$ [25] for the leading order hadronic contribution to the muon spin precession frequency within the Standard Model [26].

A remarkable consequence of this resolution of the tension is that it can be tested in a relatively straightforward fashion. Flipping the magnetic storage ring over the muon beamline, such that the muons circulate with the opposite sense around the ring, would yield a spin precession frequency in tension with the present experimental world average by $2\Delta a_\mu(\text{Exp})/a_\mu(\text{Exp}) = 2 \times (2.71 \pm 0.17) \text{ BNL} = (5.4 \pm 0.3) \text{ BNL}$, where $1 \text{ BNL} = 0.54 \text{ ppm}$ [26] is the precision achieved at BNL E821 [4] and is the precision that can be achieved at FNAL E989 [2, 3] in a data collecting run with the flipped ring lasting roughly one month. The uncertainty of the present world average, roughly 0.4 BNL [2, 26], combines with the statistics-dominated uncertainty of such a short run to give an expected significance of the tension $(5.1 \pm 0.3)\sigma$ that surpasses the conventional threshold for the discovery of a new phenomenon in particle physics, where $\sigma \approx 1 \text{ BNL}$ is the uncertainty of the comparison.

Making Axions in Polar Materials with Infrared— Axions from the local dark matter halo of the galaxy can be seen in the mid-infrared electromagnetic response of a wide range of polar materials such as silicon nitride Si_3N_4

[27]. The incoming mid-infrared light with frequency $\omega_{A\theta} = \omega_A - \omega_\theta$ makes axions within the polar material with energy $\hbar\omega_A = m_A c^2 = h \times (122.7 \pm 1.0) \text{ THz}$ by absorbing a transverse optical phonon at the far-infrared frequency $\omega_\theta \approx 2.4 \text{ THz}$ [27]. The axions leave the material and create a dip in the infrared transmission through the sample at the axion resonance frequency $\omega_{A\theta}$.

Measuring the mid-infrared frequency $\omega_{A\theta} = \omega_A - \omega_\theta$ at which the polar material makes axions and the far-infrared frequency ω_θ of the transverse optical phonons, one finds the rest-mass energy of the axion $m_A c^2 = \hbar\omega_A = \hbar(\omega_{A\theta} + \omega_\theta)$. The size of the dip in mid-infrared transmission through a sample of the polar material on the axion resonance at $\omega_{A\theta}$ is set by the infrared absorption coefficient [28]:

$$\alpha(\omega_{A\theta}) = \alpha(\omega_\theta) \frac{\Gamma_{A\theta}}{\Gamma_\theta} \frac{\omega_\theta}{\omega_{A\theta}}, \quad (8)$$

where $\alpha(\omega_\theta)$ is the absorption coefficient of the phonon, $\Gamma_{A\theta} \approx 2\pi c/t$ gives the width of the axion resonance in terms of the thickness of the sample t , and Γ_θ is the width of the phonon resonance.

Using typical parameters for a polar material such as silicon nitride Si_3N_4 , we find the mid-infrared absorption coefficient at $\omega_{A\theta}$ from the axion resonance [27]

$$\alpha(\omega_{A\theta}) = 4.0 \times \alpha(\omega_\theta) \left(\frac{t}{5 \text{ } \mu\text{m}} \right)^{-1} \left(\frac{\Gamma_\theta/2\pi c}{10 \text{ cm}^{-1}} \right)^{-1} \times \left(\frac{\omega_\theta/2\pi c}{80 \text{ cm}^{-1}} \right) \left(\frac{\omega_{A\theta}/2\pi c}{4016 \text{ cm}^{-1}} \right)^{-1}. \quad (9)$$

The mid-infrared absorption with coefficient $\alpha(\omega_{A\theta}) \approx 4\alpha(\omega_\theta)$ in polar materials such as silicon nitride Si_3N_4 at frequency $\omega_{A\theta} = \omega_A - \omega_\theta$ due to creation of axions can thus be seen with readily available samples and infrared spectrometers provided the spectrometer sees the dip with absorption coefficient $\alpha(\omega_\theta)$ in the far-infrared transmission spectrum at frequency ω_θ from the transverse optical phonon in the sample [27].

Axion Resonance in Quartz Raman Spectroscopy— A tentative observation of the axion resonance in the mid-infrared electrodynamics response of quartz (SiO_2) [29] has been reported by the RRUFF project [30] using Raman light scattering spectroscopy (Fig. 2). The scattered light intensity has a broad peak centered on the frequency shift $\omega_A(\text{SiO}_2) = 2\pi c \times (4080 \pm 4) \text{ cm}^{-1}$ which falls within the predicted window $\omega_A = m_A c^2/\hbar = 2\pi c \times (4096 \pm 32) \text{ cm}^{-1}$. Quartz has no known Raman-active vibration modes in this frequency range and chemical analysis suggests that the sample has insufficient concentration of luminescent impurities to account for the strength of the observed resonance [29].

Assuming that visible light incident on the quartz crystal makes axions within the sample, the frequency shift of the scattered light where the intensity peaks $\omega_A(\text{SiO}_2)$

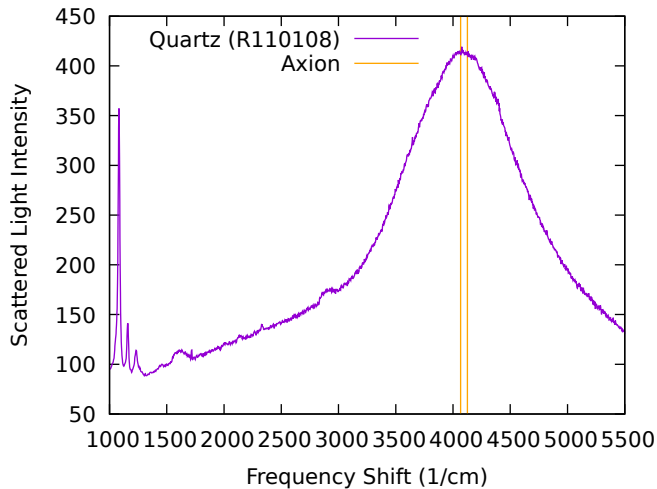


FIG. 2. Tentative observation of the axion resonance in the Raman light scattering spectrum of synthetic quartz crystal (SiO_2 , RRUFF deposition R110108) [29, 30] at room temperature and ambient pressure. The axion rest-mass (See Eq. 2) gives the window (vertical lines) for the frequency shift $\omega_A = m_A c^2 / \hbar = 2\pi c \times (4096 \pm 32) \text{ cm}^{-1}$ of visible light that makes axions within the polar material. A broad band of scattered light intensity is observed with the peak frequency shift falling within the predicted axion resonance window.

can be interpreted in terms of the rest-mass energy of the axion:

$$m_A(\text{SiO}_2)c^2 = \hbar\omega_A(\text{SiO}_2) = (0.5059 \pm 0.0005) \text{ eV}. \quad (10)$$

This agrees with the estimate in Eq. (2) but is roughly ten times more precise. If this interpretation is confirmed, then it would provide strong support for the novel physical picture of dark matter in terms of axions with number density $n_A = 6n_\gamma$.

Indeed, the rest-mass energy of the axion from quartz in Eq. (10), when combined with the axion number density $n_A = 6n_\gamma = (2464.2 \pm 1.6) \text{ cm}^{-3}$ [8] suggested by the novel physical picture of dark matter, gives the cosmological energy density parameter for axions:

$$\Omega_A h^2(\text{SiO}_2) = \frac{8\pi G}{3} \frac{h^2}{H_0^2} n_A m_A = (0.11831 \pm 0.00008), \quad (11)$$

where, $H_0/h = 100 \text{ km}/(\text{sec} \cdot \text{Mpc}) = 1/(9.778 \text{ Gyr})$ [8] gives the conventional parameterization of the present expansion rate of the universe. This agrees with the best estimate for the cosmological energy density parameter of dark matter $\Omega_A h^2 = (0.11882 \pm 0.00086)$ [10]. However, it is ten times more precise.

Conclusion— We conclude that the tensions between measurements of muon spin precession and standard model calculations are due to axions from the local dark matter halo of the galaxy. The resolution of the muon tension rests on a novel physical picture for the nature of

dark matter. The picture leads to percent level predictions for the mass of the axion and for its coupling to electromagnetic fields which can be tested using a tabletop experiment with readily available materials and devices.

Acknowledgements— The author acknowledges the support of Daria Mazura.

* nbrayali@gmail.com

- [1] J. Schwinger, Phys. Rev. **73**, 416 (1948).
- [2] D. P. Aguillard et al., Phys. Rev. Lett. **131**, 161802 (2023).
- [3] B. Abi et al., Phys. Rev. Lett. **126**, 141801 (2021).
- [4] G.W. Bennett et al., Phys. Rev. D **73**, 072003 (2006).
- [5] F. Jegerlehner, *The Anomalous Magnetic Moment of the Muon*, 2nd ed., Springer-Verlag, Berlin (2017).
- [6] The axions A_M are constructed to transform under C , P , and T as follows:

$$CA_M = A_M, PA_M = -A_M, TA_M = -A_M. \quad (12)$$

To check that they do so, recall that quarks and leptons M_H^P transforms as follows:

$$CM_H^P = \overline{M}_H^P, PM_H^P = M_H^{\overline{P}}, TM_H^P = \overline{M}_H^{\overline{P}}. \quad (13)$$

- [7] For anti-matter, the meaning of the parity check is reversed compared to matter: $P = +$ indicates anti-quarks and anti-leptons which *do* feel the weak force, while $P = -$ means the anti-matter *does not* feel it. Nevertheless, the standard model correlation between helicity $H = L, R$ and parity check $P = +, -$ applies in the same way to anti-matter as it does to matter: \overline{M}_L^- and \overline{M}_R^+ occur in the standard model while neither \overline{M}_L^+ nor \overline{M}_R^- do. See, for example, the discussion in Ref. [31] on pgs. 704–705.
- [8] There are $|M| = 12$ flavors of matter in the standard model of particle physics. They fall into three “generations” each containing a pair of quarks and a pair of leptons. See the discussion in Ref. [31] on pgs. 703–705, 707, and 721 for a detailed description of the matter content of the Standard Model in the language of quantum field theory. The ratio of the energy density parameters $\Omega_A h^2 / (\Omega_\gamma h^2) = u_A / u_\gamma$ gives the ratio of the energy per volume $u_A = m_A c^2 n_A$ stored in dark matter to the energy per volume $u_\gamma = 2.701 \times n_\gamma k T_\gamma$ stored in light energy. For a derivation, see P. J. E. Peebles, *Principles of Physical Cosmology*, Princeton University Press, Princeton, NJ (1993), pgs. 137–138, 158–160.
- [9] D. J. Fixsen, Astrophys. J. **707**, 916 (2009).
- [10] N. Aghanim, Y. Akrami, M. Ashdown, J. Aumont, C. Baccigalupi et al. (Planck Collaboration), Planck 2018 Results VI. Cosmological Parameters, A&A **641**, A6 (2018). See Planck 2018 Results: Cosmological Parameter Tables, Baseline likelihood combinations PDF tables with 68% limits, pg. 49 (May 14, 2019).
- [11] D. J. Fixsen, The Temperature of the Cosmic Microwave Background, Astrophys. J., **707**, 916 (2009).
- [12] The axion-photon coupling is given by the following expression [13, 32]:

$$g_{A\gamma\gamma} = C_{A\gamma} \frac{\alpha}{2\pi} \frac{1}{f_A} = (0.68 \pm 0.02) \times 10^{-10} \text{ GeV}^{-1}. \quad (14)$$

The rest-mass energy of the axion $m_A c^2$ and the product $m_A c^2 f_A = \sqrt{\chi_{\text{QCD}}}$ which is fixed by the topological susceptibility χ_{QCD} of the quantum chromodynamic vacuum combine to give the axion decay constant [33]:

$$f_A = \frac{m_A c^2 f_A}{m_A c^2} = \frac{(5.69 \pm 0.05) \times 10^{-3} \text{ GeV}^2}{(0.508 \pm 0.004) \text{ eV}} = (1.120 \pm 0.010) \times 10^7 \text{ GeV}. \quad (15)$$

Finally, the light quark mass ratio $m_u/m_d = 0.485 \pm 0.019$ [34] gives the dimensionless constant [13, 32]:

$$C_{A\gamma} = \frac{8}{3} - \frac{2}{3} \frac{4m_d + m_u}{m_d + m_u} = 0.653 \pm 0.017. \quad (16)$$

- [13] The axion ϕ_A couples to photons via the term in the action ($\hbar = c = 1$)

$$\mathcal{S}_{A\gamma} = \int d^3x dt g_{A\gamma\gamma} \phi_A \mathbf{E} \cdot \mathbf{B} \quad (17)$$

where, \mathbf{E} is the electric field and \mathbf{B} is the magnetic field. We follow here the conventions of Ref. [32] in which the “free” terms in the axion action take the form ($\hbar = c = 1$)

$$\mathcal{S}_A = \int d^3x dt \left[(1/2)(\partial_t \phi_A)^2 - (1/2)(\nabla \phi_A)^2 - (1/2)m_A^2 \phi_A^2 \right]. \quad (18)$$

- [14] J. Schwinger, Phys. Rev. **82**, 664 (1951). See Appendix B for the calculation of the spin precession frequency using the photon propagator $D_+(x, x')$ at leading order in quantum electrodynamics.
- [15] The photon propagator enters linearly in the quantum electrodynamic expression for the mass operator $M(x, x')$ of the muon interacting with its proper radiation field and the external magnetic field. The axion shift $\Delta D_+(x, x')$ of the photon propagator then carries over to a shift of the mass operator $\Delta M(x, x') = m_A^2 c^4 g_{A\gamma\gamma} \tilde{\phi}_A(q_A) M(x, x')$. In turn the spin precession frequency as well as the leading order quantum electrodynamic contribution to the rest-mass must shift in the same manner. They are simply the leading terms in the mass operator obtained by expanding $M(x, x')$ to leading order in the electromagnetic fine-structure constant $\alpha \approx 1/137$ [14].
- [16] A.-C. Eilers, D. W. Hogg, H.-W. Rix, and M. K. Ness, *Astrophys. J.* **871**, 120 (2019).
- [17] Under C , PT and CPT , the shift Δa_μ , like the axion amplitude, does not change sign.
- [18] For the muon beam at Fermilab E989 (FNAL) [2, 3], the volume is

$$V_\mu = 2\pi^2 R \sigma_x \sigma_y = 3.12 \times 10^4 \text{ cm}^3, \quad (19)$$

where, $R = 711 \text{ cm}$ is the radius of the central orbit of muons in the ring, $\sigma_x = 1.78 \text{ cm}$ is the radial width of the beam, and $\sigma_y = 1.25 \text{ cm}$ is the vertical width [3, 35, 36]. The average number of muons is

$$N_\mu = \frac{4}{9} N_0 e^{-t_{\text{fill}}/(\gamma\tau_\mu)} \approx \frac{4}{9} \times 4340 = 1930, \quad (20)$$

where, $N_0 \approx 6920$ is the number of muons in the ring at the start of the fill, and $t_{\text{fill}} \approx 30 \mu\text{sec}$ is the time it takes to fill the ring [3, 35]. The muon life-time in the haloscope rest frame is $T_\mu = \gamma_\mu \tau_\mu = 64.4 \mu\text{sec}$, where, $\gamma_\mu \approx p_\mu/(m_\mu c) = 29.3$ is the muon time dilation factor, $p_\mu = 3.10 \text{ GeV}/c$ is the muon momentum,

$m_\mu = 0.106 \text{ GeV}/c^2$ is the muon rest mass, and $\tau_\mu = 2.20 \mu\text{sec}$ is the muon life-time at rest [3]. For the measurements at Brookhaven E821 (BNL) [4], we estimate $N_\mu = 1290$, $\sigma_x = 2.10 \text{ cm}$, $\sigma_y = 1.53 \text{ cm}$ (J. Mott, private communication). To find the shift of muon spin precession from halo axions, we first compute $\Delta a_\mu(\text{FNAL}) = (171 \pm 10) \times 10^{-11}$ and $\Delta a_\mu(\text{BNL}) = (167 \pm 10) \times 10^{-11}$ for each experiment using Eq. (3). Next we take the average of the two experiments to obtain Δa_μ , since the shifts essentially agree. The averages are weighted by the precision of the experiments: $\sigma_{a_\mu}(\text{BNL})/a_\mu = 540 \text{ ppm}$ [4] and $\sigma_{a_\mu}(\text{FNAL})/a_\mu = 200 \text{ ppm}$ [2].

- [19] T. Aoyama et al., Phys. Rep. **887**, 1 (2020).
- [20] Sz. Borsanyi et al., Nature **593**, 51 (2021).
- [21] F. V. Ignatov et al., arXiv: 2302.08834 [hep-ex].
- [22] M. Fujikawa et al., Phys. Rev. D **78**, 072006 (2008).
- [23] S. Schael et al., Phys. Rept. **421**, 191 (2005).
- [24] M. Davier, A. Hoecker, B. Malaescu, C.-Z. Yuan, and Z. Zhang, Eur. Phys. J. C **74**, 2803 (2014). For the result $a_\mu^{\text{HLO}}(\rho^\pm) = (703.0 \pm 4.4) \times 10^{-10}$, see Ref. [19], pg. 32 below Eq. (2.13).
- [25] The consensus consists of the lattice quantum chromodynamic result $a_\mu^{\text{HLO}}(\text{QCD}) = (707.5 \pm 5.5) \times 10^{-10}$ [20] from the BMW collaboration, the dispersive result from the charged ρ^\pm vector meson resonance $a_\mu^{\text{HLO}}(\rho^\pm) = (703.0 \pm 4.4) \times 10^{-10}$ [22–24] from the BELLE and ALEPH collaborations, and the dispersive result from the neutral ρ^0 vector meson resonance $a_\mu^{\text{HLO}}(\rho^0) = ((379.5 \pm 3.0) + (322.5 \pm 2.9)) \times 10^{-10} = (702.0 \pm 5.9) \times 10^{-10}$ from the CMD-3 collaboration on resonance (first term) [21] and a recent compilation of off-resonant measurements (second term) [24]. These determinations are independent and mutually consistent. The weighted average gives the Standard Model value for the leading order hadronic contribution to muon spin precession $a_\mu^{\text{HLO}}(\text{SM}) = (704.1 \pm 3.0) \times 10^{-10}$.
- [26] The measurements from Runs 2 and 3 at Fermilab E989 [2] dominate the current world average for the muon spin precession frequency from experiment [2–4]

$$a_\mu(\text{Exp}) = (116\,592\,059 \pm 22) \times 10^{-11}. \quad (21)$$

The emerging consensus for the hadronic contribution $a_\mu^{\text{HLO}}(\text{SM}) = (7041 \pm 30) \times 10^{-11}$ [25] gives the best present estimate of the muon spin precession frequency within the Standard Model [19–24]

$$a_\mu(\text{SM}) = (116\,591\,919 \pm 35) \times 10^{-11}. \quad (22)$$

These estimates of the muon spin precession frequency create 3.4σ tension

$$\begin{aligned} a_\mu(\text{Exp}) - a_\mu(\text{SM}) &= (116\,592\,059 \pm 22) \times 10^{-11} \\ &- (116\,591\,919 \pm 35) \times 10^{-11} \\ &= (140 \pm 41) \times 10^{-11}. \end{aligned} \quad (23)$$

- [27] R. A. Nyquist and R. O. Kagel, *Infrared Spectra of Inorganic Compounds* (Academic Press, New York, NY 1971), pg. 114–115, Spectrum 134, Silicon nitride Si_3N_4 .
- [28] The absorption coefficient $\alpha(\omega)$ for electromagnetic waves of frequency ω gives the attenuation rate for the decrease of the transmitted light intensity $I(z) = I_0 \exp(-\alpha(\omega)z)$ as a function of the thickness z of the

sample for incident light with intensity I_0 . See M. Dressel and G. Gruner, *Electrodynamics of Solids*, Cambridge University Press, Cambridge, UK (2002), pg. 26. The ratio of absorption coefficients $\alpha(\omega_{A\theta})/\alpha(\omega_\theta) = |A_\theta/A_{A\theta}|^2$ is given by the ratio of the resonant amplitudes of the electromagnetic vector potential A_θ at frequency ω_θ and $A_{A\theta}$ at frequency $\omega_{A\theta}$. These amplitudes satisfy the coupled equations of motion [13]

$$\begin{aligned} i\frac{\Gamma_{A\theta}}{\omega_{A\theta}}A_{A\theta} &= g_{A\gamma\gamma}\omega_{A\theta}\omega_\theta\tilde{\phi}(q_A)A_\theta \\ i\frac{\Gamma_\theta}{\omega_\theta}A_\theta^* &= g_{A\gamma\gamma}\omega_{A\theta}\omega_\theta\tilde{\phi}(q_A)A_{A\theta}^*, \end{aligned} \quad (24)$$

which have solution $|A_\theta/A_{A\theta}|^2 = (\Gamma_{A\theta}/\Gamma_\theta)(\omega_\theta/\omega_{A\theta})$.

- [29] Synthetic quartz crystal, RRUFF project deposition R110108, <https://rruff.info/R110108>.
- [30] The Raman spectrum was collected as part of the RRUFF project (<https://rruff.info>) at room temperature (293 K) and ambient pressure (101 kPa) from a randomly oriented crystal sample on a Thermo-Almega micro-Raman system, using a 532 nm solid-state laser

with a thermo-electrically cooled charged coupled device detector. The laser was partially polarized with a 4 cm^{-1} resolution, 1 mm spot size, and 150 mW power. For an overview of the RRUFF project, see B. Lafuente, R. T. Downs, H. Yang, and N. Stone, The power of databases: the RRUFF project, in T. Armbruster and R. M. Danisi, eds., *Highlights in Mineralogical Crystallography* (Berlin, Germany, W. De Gruyter, 2015), pp. 1-30.

- [31] M. E. Peskin and D. V. Schroeder, *An Introduction to Quantum Field Theory*, Perseus, Cambridge, MA (1995).
- [32] R. D. Peccei, in *CP Violation*, ed. C. Jarlskog, World Scientific, Singapore (1989), pgs. 525–532.
- [33] M. Gorghetto and M. Villadoro, *J. High Energ. Phys.* **2019**, 33 (2019).
- [34] Z. Fodor, C. Hoelbling, S. Krieg, L. Lellouch, T. Lippert, A. Portelli, A. Sastre, K. K. Szabo, and L. Varnhorst, *Phys. Rev. Lett.* **117**, 082001 (2016).
- [35] T. Albahri et al. *Phys. Rev. Accel. Beams* **24**, 044002 (2021).
- [36] T. Albahri et al., *Phys. Rev. D* **103**, 072002 (2021) .